Cable-Driven Soft Robotic Pipe Crawler

Peter Mnev
Dept. of Robotics
University of Michigan
Ann Arbor, MI
pmnev@umich.edu

John Saunders
Dept. of Robotics
University of Michigan
Ann Arbor, MI
johnsaun@umich.edu

Aaron Tran
Dept. of Robotics
University of Michigan
Ann Arbor, MI
aartran@umich.edu

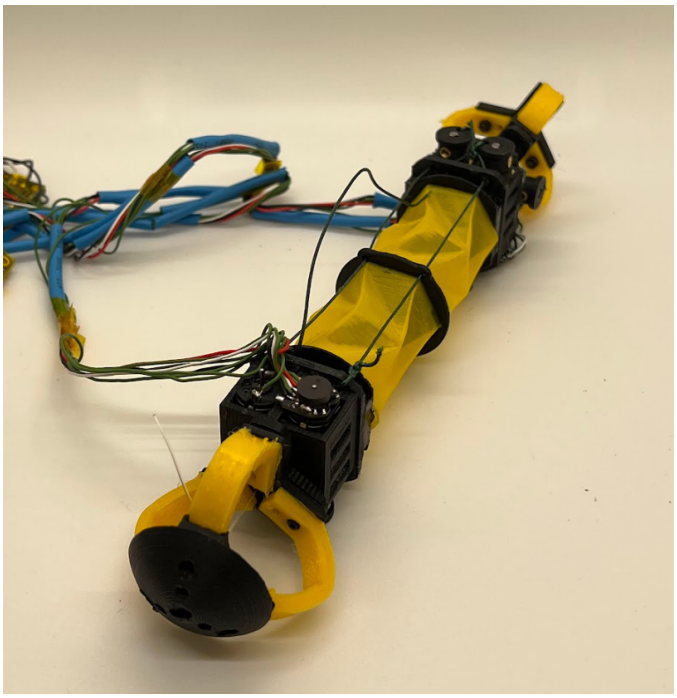
Hersh Vakharia
Dept. of Robotics
University of Michigan
Ann Arbor, MI
hershv@umich.edu

***Abstract*—Soft robots have been gaining popularity in recent years due to their ability to adapt to complex environments and tasks. Additionally, soft robots have emerged as a promising solution for navigating through confined spaces, such as pipes. In this paper, we present a cable-driven soft robot capable of autonomous pipeline traversal using earthworm-style locomotion. The robot is comprised of a body made of Kresling geometry, as well as two end-pieces that contain soft C-springs. The body and C-springs are compressed with cables actuated by high-torque motors. This robot was designed to compete in tasks that emulate the 2023 RoboSoft competition, in which a soft robot is required to traverse pipes in various configurations. Our results from testing show the robot is able to successfully move along straight paths at any incline but struggled moving through turns. However, we believe that, with improvements, this design can be very effective for autonomous pipeline navigation and has high potential to be untethered.**

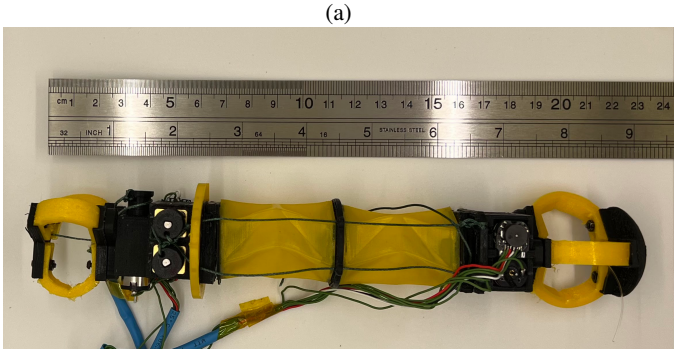
I. Introduction

Researchers across the globe continue to investigate the application and implementation of flexible and deformable materials such that soft robotic systems can interact with environments in a more natural and adaptable way than traditional rigid-body mechanisms. The potential for soft robotics to revolutionize human-robot-interaction and operation is becoming increasingly apparent as the field continues to develop. Advancements in materials science, manufacturing techniques, and control systems have rapidly expanded soft robotics into a vast range of applications, such as search and rescue operations, terrain traversal, and exploration.

Various iterations of earthworm-style robotic crawlers exist for in-plane locomotion through pipe and tube environments [1]–[3]. These soft robotic systems are often designed to move through tight spaces and over rough terrain using flexibility and adaptability to navigate unknown environments. Some published designs feature pneumatic actuation for locomotion [1], [2], while others rely on directional actuation of magnetic fields to create motion [3]. While pneumatic soft robotic mechanisms have proven to be effective, the pneumatic assemblies are often too large and bulky to allow for on-board mounting to the crawlers, thus preventing untetherability and scaled down sizing. Magnetic systems can avoid the problem of bulkiness and allow for small scalability. However, reliance on large magnetic field generation surrounding the robot often prevents these systems from being reliable outside of a controlled lab environment.



(a)



(b)

Fig. 1: (a) Proposed cable-driven soft robotic pipe crawler assembly and (b) its length measurement for scale when compared to published designs.

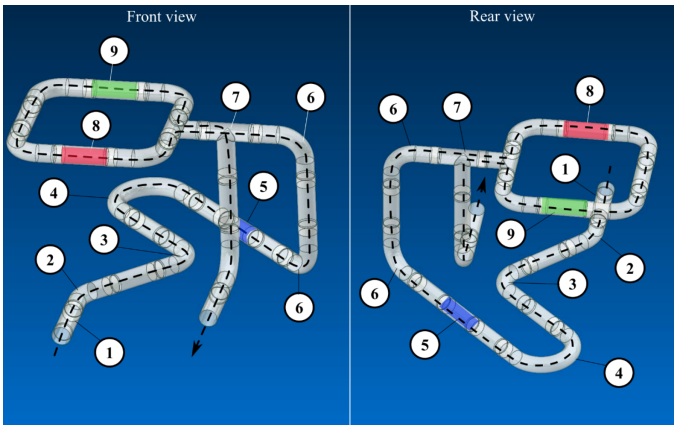


Fig. 2: RoboSoft Competition 2023 terrestrial race course diagram with labeled navigation sections [4].

We propose a cable-driven soft robotic crawler capable of autonomous locomotion and pipeline traversal, shown in Fig. 1. The proposed robotic system is designed to compete in a competition setting that emulates test conditions from the 2023 RoboSoft Competition scenarios and rules [4]. The RoboSoft terrestrial race features deployment of a robot into a pipeline that requires inspection. For the terrestrial race scenario, the robot must autonomously navigate the pipeline and exit for potential data recovery. Fig. 2 displays a 3D model of the proposed RoboSoft competition pipeline course for 2023. The nine competition tasks and corresponding labeled sections are defined as follows:

1) The robot starts on a horizontal straight pipe.
2) A 45-degree turn.
3) A 90-degree turn.
4) A U-turn.
5) An obstructed sector: the diameter of the pipe is reduced by 50%.
6) A 90-degree turn upward, followed by a vertical straight pipe, followed by another 90-degree turn back to horizontal straight pipe.
7) A two junction: the robot has to go straight initially, then turn to complete one of the branches proposed. It is not required to follow a specific order.
8) Pipeline has 5 mm silicone walls, unable to provide a solid wall to push against.
9) Pipeline has a dirty sector to simulate realistic pipes, concludes with the selection and exit from the last tract.

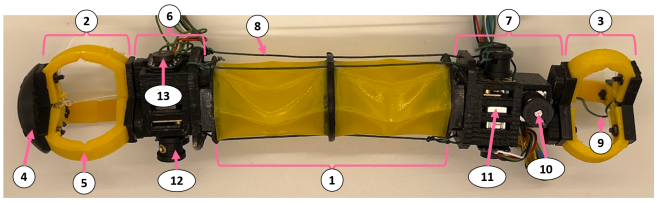
The structure of this paper is as follows: Section II describes the project methodology, Section III communicates the experimental results, and Section IV discusses the importance of the results and the conclusions drawn from experimentation.

II. Methodology

This section details the methodology behind the cable-driven pipe-crawling robot, including an overview of the mechanism and electronics designs, descriptions of robot locomotion cycle, the fabrication methods for assembly, and the experimental setup for testing.

A. Design Overview

The final mechanical and electrical assembly of the origami robotic pipe-crawler is shown in Fig. 3. The mechanical assembly features five modules that can be detached and modified in dimension: one Kresling origami body, two motor housing attachments, and two C-spring end-pieces. A combination of five motors with cable reels is the driving force behind robot compression and extension to exhibit locomotion.



1 – TPU95A Kresling origami body
2 – Front end-piece module
3 – Rear end-piece module
4 – PLA nose attachment
5 – TPU95A C-spring
6 – Front PLA motor housing
7 – Rear PLA motor housing
8 – Body cable
9 – C-spring cable
10 – C-spring motor
11 – Body motor
12 – PLA cable reel
13 – Motor encoder

Fig. 3: Fully assembled soft robotic crawler.

1) Kresling Origami Body: The Kresling Origami Structure is a type of origami tessellation developed and studied by Biruta Kresling [5]. The Kresling pattern features a series of mountain and valley folds that create a contracting and expanding zig-zag pattern. Interlocking spirals are formed when the zig-zag patterns are folded together to create a standing 3D structure. A example of the 2D Kresling origami pattern on an origami sheet is shown in Fig. 4.

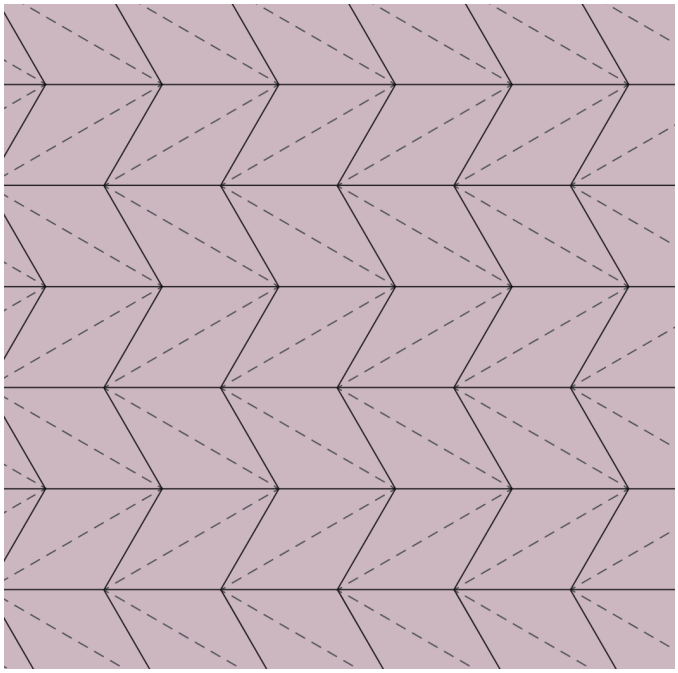


Fig. 4: 2D Kresling origami pattern sheet [6].

The 3D Kresling spiral structure can contract and expand by twisting one face and letting the geometry fold in on itself. In this motion, the other face of the structure remains

stationary. Combining two Kresling spiral units into a dipole with mirrored orientations allows the inner faces of the dipoles to twist while the outside faces remain stationary. Fig. 5 shows a representation of the Kresling unit and its contraction when formed into a dipole [3].

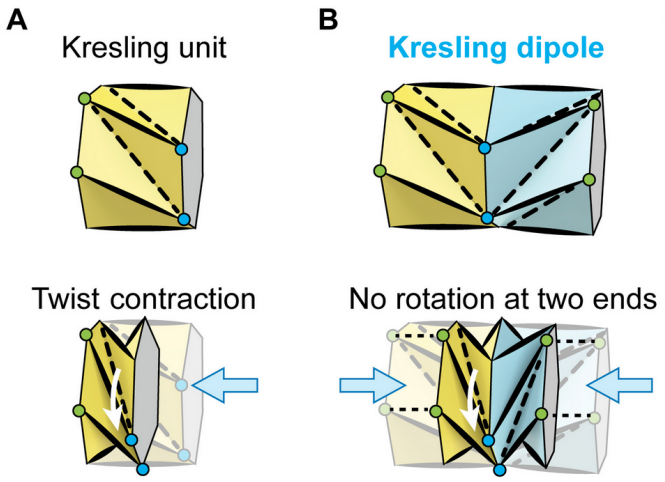


Fig. 5: Kresling unit and dipole contraction [3].

Effective implementation and demonstration of locomotion and actuation using the Kresling origami structure has been documented by prior research groups [3], [5], [7]–[10]. Complex systems such as robotic arms and worm-style crawlers can be utilized based on the controlled twist, extension, and compression of Kresling units in sequence. The Kresling unit geometry used in the main body of the cable-driven assembly emulates dimensions experimentally examined for a vaccum actuated Kresling arm [8]. Fig. 6 contains the geometric dimensions used in fabrication of the Kresling body modules.

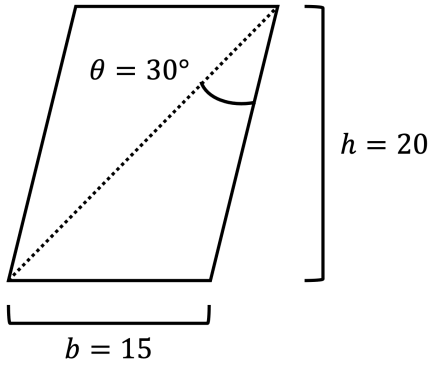


Fig. 6: 2D geometry of a parallelogram contained within the Kresling origami pattern, length measurements in [mm].

2) C-Spring End-Piece Modules: Each end-piece module features three C-springs mounted to two 3D printed PLA plates. The front end-piece module has an additional "nose" attachment to provide additional aid in guiding the front of the crawler while moving in the pipeline. C-spring expansion under compression allows the end-piece modules to provide normal force and friction to the inner walls of the pipeline. When compressed, the end-pieces hold the crawler in place to allow compression of the Kresling body and locomotion. Fig. 7 shows the geometry of the C-spring modules when subject to a force.



(a) (b)

Fig. 7: (a) C-spring end-piece module extended and (b) the same module when compressed by the motor and cable reel.

3) Electronics: The robot uses five motors total - three 75:1 motors for compressing the Kresling body, and one 380:1 for each C-spring end-piece. The motors are Micro Metal 6V high-powered brushed DC gearmotors from Pololu, which feature a combination of high-torque and small form factor [11]. The motor speed produced is not important, but rather having a gear ratio to produce sufficient torque to compress the body and C-springs is necessary. However, the motors are still reasonably fast in operation. Each body motor is equipped with a 12 CPR magnetic encoder to allow precise position control. The encoders are necessary for accurate body compression, as each body motor needs to spool the cables by the same amount.

The Adafruit TB6612FNG motor driver board controls the electronics boards [12]. Each of these boards can drive 2 DC motors, resulting in 3 boards total for use. Each motor can be controlled through the TB6612FNG board with 3 pins: 2 pins dictate the direction the motor is spinning, and the third pin is a PWM to set the motor speed.

The main control board is a Raspberry Pi Pico W [13]. The RPi Pico W board offers a small form factor with 26 multi-purpose GPIO pins. Each GPIO pin can be configured as an external interrupt, a feature highly important for operation. The encoders require 2 interrupts each for the most accurate position data; the Pico W offers enough interrupts to have encoders for all body motors, while a board such as the Arduino Nano, which only has 2 external interrupts, does not. The RPi Pico W board can also be programmed with MicroPython, allowing for useful abstractions when prototyping. Additionally, it has built-in WiFi communication, offering the potential for untethered operation.

To power the system, two 3.7 V 300 mAh batteries are utilized. They are wired in series to provide the 7.4V sufficient for powering the motors. A single battery of the pair can be used to power the Pico W, although the Pico W was powered

through USB connection during testing. The board can easily be powered when future developments enable untethered movement using the Pico W's onboard WiFi communication.

A full schematic of the electronics and communication paths can be found in Appendix A.

B. Locomotion Cycle

The locomotion cycle for moving the robotic crawler through a pipeline follows the specified Algorithm 1 based on the end-piece and Kresling body module structure. At least one C-spring end-piece module must be inserted into the pipeline for the locomotion cycle to begin. Fig. 8 shows the locomotion cycle performed by the robotic crawler outside of the pipe to aid in visual representation.

Algorithm 1 Robotic Crawler Locomotion Cycle

1: Compress front end-piece module.
2: Compress Kresling body module.
3: Compress rear end-piece module.
4: Release front end-piece module.
5: Release Kresling body module.
6: Compress front end-piece module.
7: Release rear end-piece module.
8: Repeat Steps 2-6

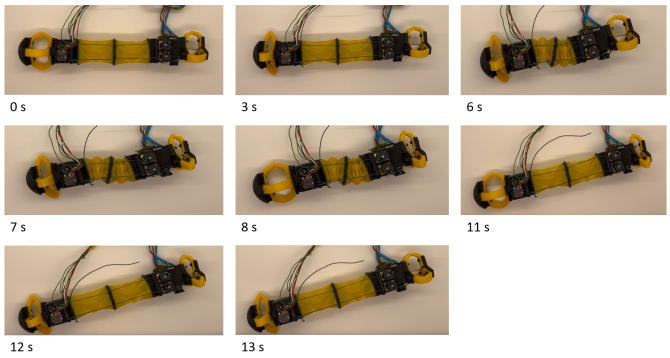
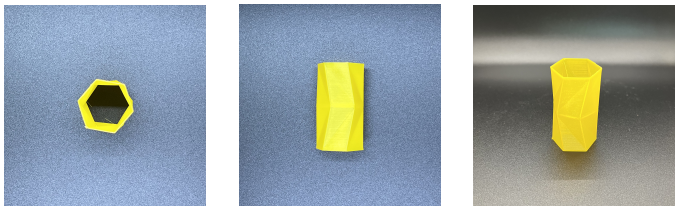


Fig. 8: Locomotion cycle of pipe-crawler representation outside of pipeline system, demonstrating Algorithm 1.

C. Fabrication Method

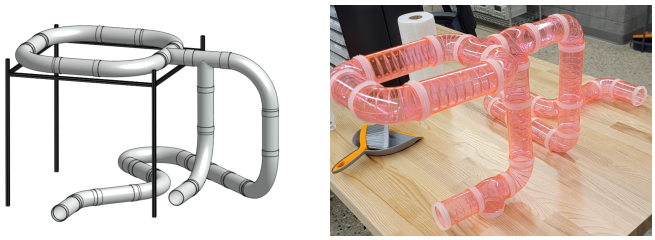
The material selected for 3D printing Kresling origami body modules and individual C-springs is PolyFlex™TPU95 [14]. PolyFlex™TPU95 is a thermoplastic polyurethane (TPU) based filament that features a shore hardness of 95A. This particular filament can stretch upwards of three times its original length, providing ample springback when undergoing compression. Fig. 9 shows multiple views of a 3D printed Kresling body from the Ultimaker S5 using PolyFlex™TPU95.

The motor housings, nose attachment, and cable reels are all printed with standard PLA to provide structure and rigidity. The motor housings also have openings to provide passive cooling to the motors during long run times.



(a) (b) (c)

Fig. 9: (a) Top view, (b) front view, and (c) isometric view of Kresling origami body module printed with PolyFlex™TPU95 on an Ultimaker S5.



(a) (b)

Fig. 10: (a) CAD model of 2023 RoboSoft pipeline course [4] compared to (b) the constructed pipeline course used in experimentation of navigation.

D. Experimental Setup

The experimental setup to test locomotion and navigation of the worm robot in confined spaces was created to emulate the terrestrial race course designed and implemented in the 2023 RoboSoft Competition, represented by the CAD model in Fig. 10a [4]. The experimental replication of the 2023 RoboSoft pipeline course subject to different pipe dimensions and characteristics is shown in Fig. 10b. The inner diameter of the pipe used for the emulated course is approximately 2" (5.08 cm), which is approximately 1.94" (4.93 cm) smaller than the inner diameter of the RoboSoft pipeline [4]. Additionally, the emulated pipeline course features a ribbed inner lining, preventing smooth locomotion along the base of pipe sections and shrinking the inner diameter by fraction. All competition sections for scoring are emulated, including the 50% diameter reduction, 5 mm silicone lining, and dirty pipe sectors.

General locomotion, compression, and spring-back testing of the Kresling origami body and C-spring end-pieces is performed using a testing setup comprised of the origami worm assembly, a Kiprim DC310S programmable DC power supply, and a laptop to run any python programs and motor commands.

III. Results

Fig. 11 shows the position of the robotic crawler while traversing a horizontal section of pipeline, emulating the requirements of Task 1 [4]. The soft robotic crawler was placed fully into the tube before running the electronics. The crawler moved its full body length horizontally through the tube, approximately 9" (22.86 cm), before being snared by

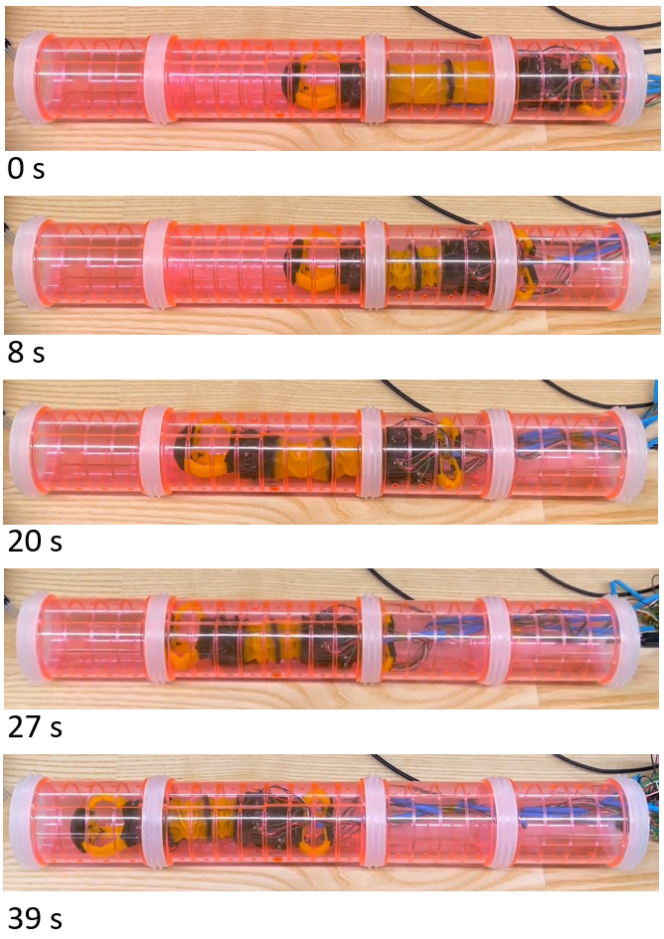


Fig. 11: Time-lapse of pipe-crawler locomotion through a straight pipe section, emulating Task 1 [4].

pipe ridges on the inner diameter. The total horizontal crawling test run time was 39 seconds, resulting in the robot crawling approximately 0.23 in/sec (0.586 cm/sec).

Fig. 12 shows the position of the robotic crawler while traversing a vertical section of pipeline, emulating the requirements of Task 6 [4]. The soft robotic crawler was placed almost fully into the tube before running the electronics, leaving only the rear end-piece outside of the pipe. The crawler moved more than its full body length vertically through the tube, continuing to climb until limited by the length of the tethered wires rather than the inner ridges of the pipe. The total run time was 104 seconds for the vertical climbing test.

Fig. 13 shows the position of the robotic crawler while traversing a 90 degree turn in the pipeline, emulating the requirements of Task 3 [4]. The soft robotic crawler was placed fully into the tube before running the electronics. The robotic crawler was not able to complete the task, getting stuck inside of the tube due to lack of steering of the front end-piece, running for a total elapsed time of 35 seconds.

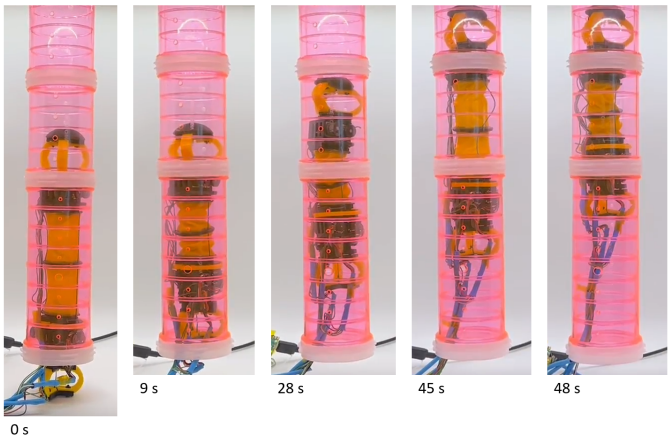


Fig. 12: Time-lapse of pipe-crawler locomotion through a vertical pipe section, emulating parts of Task 6 [4].

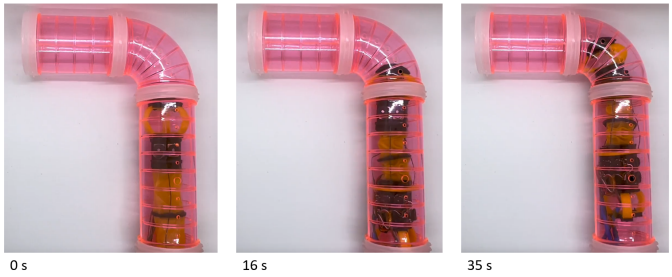


Fig. 13: Time-lapse of pipe-crawler locomotion through a 90 degree turn pipe section, emulating Task 3 [4]. The robot was not able to complete the turn, getting stuck in the final position shown.

IV. Discussion and Conclusion

The cable-driven pipe-crawling soft robot was able to demonstrate both effective horizontal and vertical locomotion inside a constricted pipeline. However, the worm robot was unable to complete the 90 degree turn inside of the pipeline. The largest limitation when tasked with pipe traversal in this experimental setup was the ridge extrusions along the inner diameter of the pipeline. Often in testing, the inner edges would snare the motor housing edges. The Kresling body module was unable to provide the force necessary to overcome the friction introduced by the inner edges of the pipe. Another issue presented by the edges involved the encoders. Certain test runs results in the encoders pushing into the inner pipe wall, stalling the motors and preventing continuation of the locomotion cycle. Timeouts were introduced to mitigate the effects of motor stalling when snared on edges, but preventing encoder pressure against the wall largely improved performance. More scenarios, such as emulating the 45 degree turn in Task 2 [4], were not tested. To complete the majority of the RobotSoft competition tasks, a number of improvements must still be made.

The Kresling body loses significant force output when bent. This poses challenges for making 90 degree turns. Considering

how forward motion occurs purely by the body's restitution, a high body stiffness is essential to the robot's functionality. Work must be done to characterize Kresling stiffness when straight and bent to support parametric design of the body. Some parameters worth considering include the number of Kreslings, Kresling length in compression and extension, Kresling angle in geometry, and Kresling base width. An increase in number of Kreslings would likely increase stiffness as it can be modeled as springs in series. Local curvature can also be reduced with more Kreslings, which would prevent buckling in each unit. However, a longer robot body may be undesirable due to complicating task initiation. The robot could potentially start with the nose in the pipes, but a long body would require starting the front of the robot further inside the pipe than may be allowed.

In addition to the Kreslings, the C-springs would benefit from characterization of the force input/output and deformation. This robot was designed with a miniaturized obstacle course compared to that of RoboSoft's [4], which is significantly larger. New C-springs that take into consideration the different diameter sizes, increased weight from scaling up the robot, and length constraints would be necessary. An optimal design can be reached by first characterizing the aforementioned behavior. This process was somewhat rushed and left up to trial and error due to time considerations for this project.

Autonomous and untethered motion is essential to both maximizing points in the competition and practical functionality in real pipe exploration. This system is currently capable of neither, though untetherability is achievable through software improvements. To make the robot untethered, only the wireless module would need to be completed. Autonomous behavior would require a camera or time of flight sensor and an IMU for pose estimation. This would enable the robot to make decisions in pipe junctions and actively turn as opposed to being guided by pipe walls. A camera would likely be better for overall information gathering, but a time of flight sensor could be desirable for more simplistic control.

Some smaller but still vital changes to the robot include: manufacturing a custom PCB; adding encoders to the end piece motors; motor mount/housing changes for modularity and assembly, motor securement, and encoder protection; and mechanical features to support cable management.

After completing the above changes, it would be desirable to evaluate performance characteristics to tune the system on a whole and understand its operating conditions. Important characteristics include but are not limited to: power consumption and battery life; maximum translational speed; optimal actuation frequency; minimum radius of curvature for curvilinear motion; and maximum carrying capacity.

REFERENCES

[1] X. Zhang, T. Pan, H. L. Heung, P. W. Y. Chiu, and Z. Li, "A biomimetic soft robot for inspecting pipeline with significant diameter variation," in *2018 IEEE/RSJ International Conference on Intelligent Robots and Systems (IROS)*, 2018, pp. 7486–7491.

[2] Z. Zhang, X. Wang, S. Wang, D. Meng, and B. Liang, "Design and modeling of a parallel-pipe-crawling pneumatic soft robot," *IEEE Access*, vol. 7, pp. 134 301–134 317, 2019.

[3] Q. Ze, S. Wu, J. Nishikawa, J. Dai, Y. Sun, S. Leanza, C. Zemelka, L. S. Novelino, G. H. Paulino, and R. R. Zhao, "Soft robotic origami crawler," *Science Advances*, vol. 8, no. 13, p. eabm7834, 2022. [Online]. Available: https://www.science.org/doi/abs/10.1126/sciadv.abm7834

[4] "Robosoft competition 2023 scenarios and rules," Aug 2022. [Online]. Available: https://softroboticsconference.org/

[5] B. Kresling, "Origami-structures in nature: lessons in designing "smart" materials," *MRS Online Proceedings Library (OPL)*, vol. 1420, pp. mrsf11–1420–oo02–01, 2012.

[6] M. Gardiner, "Kresling." [Online]. Available: https://orilab.art/natural/kresling

[7] L. Lu, X. Dang, F. Feng, P. Lv, and H. Duan, "Conical kresling origami and its applications to curvature and energy programming," *Proceedings of the Royal Society A: Mathematical, Physical and Engineering Sciences*, vol. 478, 01 2022.

[8] Z. Zhang, W. Fan, G. Chen, J. Luo, Q. Lu, and H. Wang, "A 3d printable origami vacuum pneumatic artificial muscle with fast and powerful motion," 04 2021, pp. 551–554.

[9] N. Kidambi and K. W. Wang, "Dynamics of kresling origami deployment," *Physical Review E*, vol. 101, no. 6, jun 2020. [Online]. Available: https://doi.org/10.1103%2Fphysreve.101.063003

[10] Y. Miyazawa, C.-W. Chen, R. Chaunsali, T. S. Gormley, G. Yin, G. Theocharis, and J. Yang, "Topological state transfer in kresling origami," *Communications Materials*, vol. 3, no. 1, p. 62, Sep 2022. [Online]. Available: https://doi.org/10.1038/s43246-022-00280-0

[11] "Pololu - micro metal gearmotors." [Online]. Available: https://www.pololu.com/category/60/micro-metal-gearmotors

[12] A. Industries, "Adafruit tb6612 1.2a dc/stepper motor driver breakout board." [Online]. Available: https://www.adafruit.com/product/2448

[13] "Raspberry pi pico w datasheet." [Online]. Available: https://datasheets.raspberrypi.com/picow/pico-w-datasheet.pdf

[14] "Polyflex tpu95," Apr 2023. [Online]. Available: https://us.polymaker.com/products/polyflex-tpu95

APPENDIX A
ELECTRONICS DIAGRAM

